

Chapter 11

WETLAND-WATERSHED MODELLING AND ASSESSMENT: GIS METHODS FOR ESTABLISHING MULTISCALE INDICATORS

***Javier Martínez-López, M. Francisca Carreño,
José Antonio Palazón-Ferrando, Julia Martínez-Fernández
and Miguel Ángel Esteve****

Departamento de Ecología e Hidrología, Universidad de Murcia
Campus de Espinardo, 30100-Murcia, Spain

Abstract

In the context of wetland ecosystem management, a combination of approaches involving different time and spatial scales must be applied. One primary driver of wetland degradation is agricultural expansion at watershed scale. Wetlands have undergone several hydrological and biological changes as a consequence of increased water inputs from agricultural drainage off the watershed. For the establishment of suitable wetland ecological indicators, watershed scale studies focusing on pressures influencing ecosystem dynamics are necessary. Specific enhanced methods for watershed modelling, wetland mapping and land cover assessment are thus essential tools for wetland monitoring and management.

Watershed draining to the Marina del Carmolí semiarid wetland in Murcia Region (SE Spain) was delimited using a digital elevation model. Map algebra operations were applied on the elevation model of the Campo de Cartagena coastal plain to reinforce existing drainage network and to force flow accumulation from all draining areas around wetland perimeter to converge into a single point within the wetland area. Watershed delineation was thus improved.

A land use/land cover map of the Campo de Cartagena was then obtained for year 2008-09 by means of supervised classification of Landsat images. A set of four spectral indices were calculated and included in the classification analysis using a combination of bands in order to better discriminate vegetation, water bodies, infrastructures and bare soil. An enhanced classification procedure based on maximum likelihood and random reselection of train areas was applied. Object-based analysis of the Landsat scenes based on automatic image segmentation diminished the occurrence of isolated

*E-mail address: javier.martinez@um.es

pixels in the classification. The proposed classification methodology showed great accuracy, thus improving the results of traditional classification techniques.

Wetland plant communities in Marina del Carmolí wetland were mapped in 2008 by means of remote sensing techniques using satellite and airborne images. Characteristic plant communities were first characterized by combining fieldwork sampling of plant species and multivariate analysis. Georeferenced sampling units were further used as training areas for supervised image classification of plant communities. Maps obtained showed great accuracy. However, sensors are adequate for different applications.

The proposed set of GIS methodological tools contributes to improve the study of wetland plant as indicators, the mapping and future monitoring of watershed land cover classes, and the study of wetland plant community changes over time. All pieces of software used in the study are free and mainly open source programs, which make it an inexpensive and universal methodology.

PACS 05.45-a, 52.35.Mw, 96.50.Fm.

Keywords: wetland, watershed, indicators, remote sensing, modelling.

Introduction

The Campo de Cartagena coastal plain constitutes the catchment area of the Mar Menor lagoon (figure 1). It comprises 1,275 km² of a coastal plain with a slight slope towards the Mar Menor lagoon and with some elevations up to 700 m. It is under the influence of a very arid climate with a mean annual temperature higher than 18° C and mean annual rainfall under 300 mm [12].

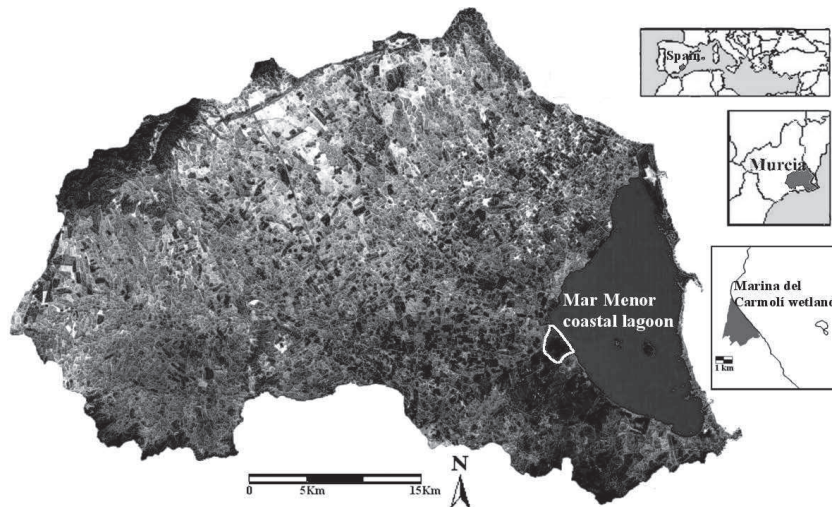


Figure 1. Mar Menor basin.

Associated to internal shore of the Mar Menor lagoon there are a series of coastal wetlands which are protected at regional, national and international level due to their high ecological value (Ramsar Site, Special Protection Area for Birds, Site of Community Importance and Special Protection Area for the Mediterranean). They are also included in

the regional inventory of wetlands [2]. The lagoon and their associated wetlands contain eighteen Habitats of Community Interest, according to the European Habitat Directive [18], being one of them of priority interest.

These Mediterranean semiarid wetlands are semi-aquatic ecosystems, *i.e.* environments between steppes and standing water ecosystems, also called crypto-wetlands. Characteristic plant communities of crypto-wetland are salt steppes and salt marshes. The salt-steppe units are mainly composed by the priority habitat 1510 "Mediterranean salt steppes, Limoni-italia" of the European Habitat Directive [20]. Main species in salt steppe are *Lygeum spartum*, *Suaeda vera*, *Frankenia corymbosa* and *Limonium caesium*. The saltmarsh units are dominated by habitat 1420 (Mediterranean and thermo-Atlantic halophilous scrubs, *Sarcocornetea fruticosi*) and habitat 1410 (Mediterranean salt meadows). Main species in salt-marsh are *Sarcocornia fruticosa*, *Arthrocnemum macrostachyum*, *Halimione portulacoides* and *Halocnemum strobilaceum*. Finally, reed beds units, when present, are dominated by *Phragmites australis*. The spatial distribution of the vegetation units depends mainly on water and salinity conditions.

Wetlands naturally act as a sink of upland occurring drainages, therefore watersheds are important elements when studying wetlands in relation to landscape hydrological changes [47]. During recent decades several land use changes in the Mar Menor watershed are threatening its conservation. The expansion of agricultural irrigated lands and urban and touristic development in the watershed have led to significant hydrological changes that affect the lagoon and their associated wetlands [19]. Plant species and communities have been often used as a tool for wetland condition assessment in relation to watershed pressures [15, 31].

GIS and remote sensing are widely used in wetland [32, 34, 40] and land use/land cover studies [1, 41, 48]. However, few studies develop enhanced specific methodologies for the study of wetland-watershed relationships in coastal areas [25].

First, watershed area draining to the Marina del Carmolí wetland was delimited using an enhanced method developed for plain areas. Secondly, land uses/cover classes in the whole Campo de Cartagena area were mapped by means of remote sensing using Landsat images. The standard supervised image classification methodology was complemented with a set of ancillary layers based on spectral and shape image indices, as well as with a procedure that minimizes classification error related to train sites intraclass heterogeneity. Finally, through fieldwork and multivariate ordination analysis wetland plant communities were characterized and mapped at 2 and 30 meters spatial resolution by means of different remote sensors. Obtained maps were compared in terms of accuracy and potentialities for wetland monitoring. All map layers and GIS analyses in this study have been processed with open source software. *GRASS* 6.4 software [24] was used for most GIS analyses, and *R* [42] was used for statistical analyses.

This chapter proposes a set of methods for a comprehensive study of wetland-watershed systems combining fieldwork and advance GIS modelling techniques. A framework for the proper establishments of indicators at different scales is presented, based on specific enhanced methods for wetland hydrological modelling, land use/land cover mapping and wetland plant communities characterization and mapping. The Marina del Carmolí wetland, on the shore of the Mar Menor lagoon was selected as a study case in coastal plain areas.

Wetland Watershed Modelling

Within the context of wetland-watersheds studies, it is necessary to determine the scale at which land uses or land cover types play a major role. Delineating specific watershed areas draining to each wetland is therefore essential for the establishment of wetland-landscape relationships, specially when studying wetlands located in nearby areas.

Standard GIS hydrological modelling modules are not always suitable for wetland watershed delineation. Several issues may arise, specially for wetlands located in plain areas, where the drainage network might no be clearly defined in a digital elevation model (DEM). Watersheds are usually delineated by the area upstream from a given outlet point. When several stream network channels drain into a wetland, their respective outlet points within the wetland must be properly identified to obtain each corresponding sub-watershed. Specially in plain areas, identifying relevant outlet points inside the wetland area can be a very time-consuming process, particularly at large wetlands. That is the case for wetlands located on the shore of the Mar Menor lagoon, since they are embedded in the Campo de Cartagena coastal plain. Enhanced methods for wetland-watershed delineation are therefore necessary.

By means of map algebra DEM was preprocessed to enhance wetland watershed delineation in the Mar Menor coastal plain. A single outlet point was created within Marina del Carmolí wetland area and the drainage network in the Campo de Cartagena coastal plain was accentuated.

A pixel in an arbitrary coordinate of the wetland area was first selected, which will ultimately serve as a sink or outlet point, from which to delineate wetland watershed. A map was created using *GRASS* command *r.distance* in which remaining pixels inside wetland area were assigned a distance value related to the selected pixel. The highest distance map value was then obtained using *GRASS* command *r.univar* and a new map was created using *GRASS* command *r.mapcalc* by subtracting this value from the former distance map values. The resulting map (figure 2) represented inverse distances with the lowest values in the wetland perimeter pixels and the highest value in the pixel selected as a sink. This map was then subtracted to the 10 meters resolution DEM of the Campo de Cartagena. DEM outside of wetland area was also modified by lowering the elevation values coinciding with existent stream network to force flow-direction models to match existing stream lines [33]. We therefore obtained a single point within the wetland area from which to perform watershed delineation in order to collect all drainage fluxes reaching the wetland perimeter and moreover, drainage network was improved with known existing stream network.

We used *GRASS* command *r.watershed* to generate maps of flow accumulation and drainage direction based on the modified DEM (figure 3). Single flow direction (D8 algorithm) method was applied for this purpose. Two main inflows coming from the watershed were identified, which converged into the previously selected sink point.

GRASS command *r.water.outlet* was finally used to obtain watershed area from the selected sink coordinate within the wetland using the drainage direction map (figure 4).

Watershed area obtained comprised 17,000 ha and was consistent with previous hydrological studies in the Campo de Cartagena coastal plain area [12]. Without the DEM preprocessing methodology applied here watershed area obtained was significantly smaller (9,318 ha) and it was necessary to try several hundred pixels within the wetland area as

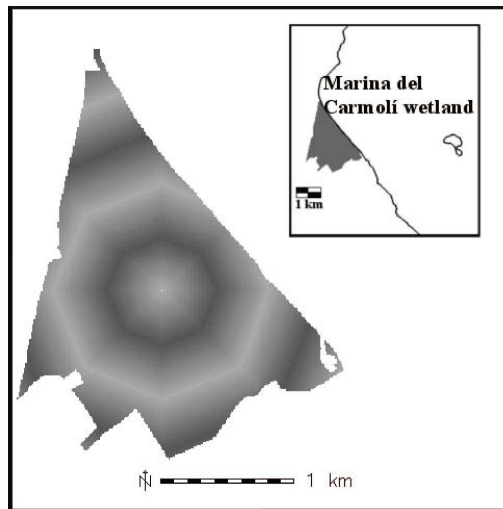


Figure 2. Modified DEM in Marina del Carmolí wetland. Sink point is the white pixel in the center of the wetland area.

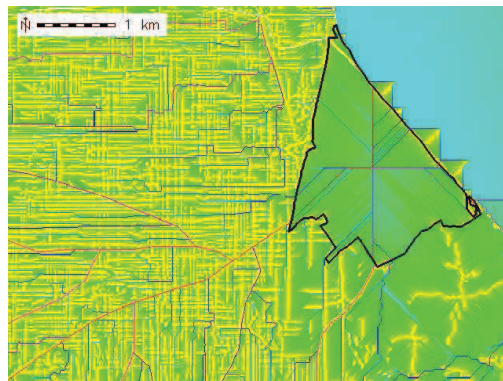


Figure 3. Logarithm of flow accumulation map with forced flow into a single point within the Marina del Carmolí wetland. Wetland boundary is denoted in black.

sink points for watershed delineation, thus making it a very uncertain and time consuming process.

Land Use/land Cover Mapping

Land use changes in wetland watersheds might lead to hydrological alterations, which directly influence plant communities in wetlands, and ultimately its associated fauna [19]. Several methodological issues arise when performing land use/land cover mapping by means of supervised classification methods.

Standard available methods do not account for neighbor pixel sets when generating classification maps, or rather they cannot see the *forest*, *i.e.* landscape patches, but only the *trees*, *i.e.* pixel sized landscape units. However, landscapes mostly consist of different patches of every land use/land cover class. Pixel based classification methods are therefore biased by

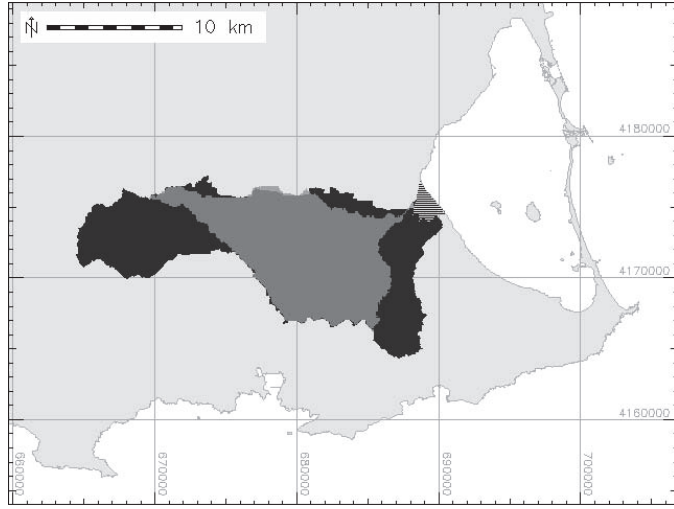


Figure 4. Watershed area of the Marina del Carmolí wetland. The watershed obtained without MDE preprocessing is denoted in gray color and the improved version is represented in black color. Marina del Carmolí wetland is the striped area on the shore of the Mar Menor Lagoon.

pixel size and lead to a high percentage of isolated pixels of different classes in the resulting map.

Train sites quality also determines classification accuracy. The selection of reliable and representative train sites sets is crucial for the proper elaboration of spectral signatures. This is specially important for land cover time series maps, for which train sites must be extracted from different sources, often of unequal quality.

Finally, distinctiveness of spectral signatures for each land use/land cover class depend also on the available remote sensor bands. However, available bands can be also combined into several indices, which enhance the discrimination of specific land cover classes.

In this section we develop a specific enhanced methodology to map land use/land cover, which minimizes the effect of train sites heterogeneity, includes patch scale information and uses a set of ancillary layers corresponding to several spectral indices.

The Landsat 7 ETM+ sensor has a spectral resolution of 7 bands, *i.e.* blue (B), green (G), red (*R*), near infrared (NIR), short-wave infrared (MIR), thermal infrared (TIR) and panchromatic (P). Pixel size of all bands is 30 meters except for the thermal infrared and panchromatic bands, which have a pixel size of 60 and 15 meters respectively.

Two Landsat images were used for classification corresponding to different dates, winter and late spring, in order to account for the changing seasonal phenology of vegetation during the dry and wet periods [5], hence enhancing the discrimination of land cover classes, specially in arid regions, like the study area. Images were obtained from the Spanish National Geographic Institute (IGN) within the frame of the National Remote Sensing Plan (PNT). Importing images into the GIS was performed by applying the GRASS command *r.in.gdal*. Pixel size was set to original image resolution.

Landsat images were georectified to the Universal Transverse Mercator coordinate system (European Datum 1950, zone 30 North). For this purpose, forty control points were

placed by comparing with a georeferenced Landsat panchromatic image of 15 m spatial resolution, dated from 2001 and covering the same area. Nearest-neighbor interpolation based on the control points was performed using a 2nd order polynomial function with *GRASS* command *i.rectify*. The root mean square error (RMSE) values achieved for all control points was lower than the pixel size. Radiometric correction was not performed since training data and the images to be classified were in the same relative scale [46].

Land use/land cover maps (LULC) were obtained by supervised classification using the maximum likelihood algorithm [37, 43]. Train and validation sites maps were obtained through aerial photo interpretation.

Eleven land cover classes were studied: dense (DNW) and open (ONW) natural woodland, dense (DNS) and open (ONS) natural shrubland, dry arboreal (DAC) and herbaceous (DHC) cropland, irrigated arboreal (IAC) and herbaceous (IHC) cropland, greenhouses (GHs), unproductive land (UNP) and water bodies (WBs).

Train sites reselection

Classification was enhanced with an iterative procedure that minimizes the effect of uncertainty and heterogeneity in the selection of train sites. This method was originally developed by González and Palazón [23] and combines *GRASS*, *R* and bash shell scripts to perform hundred supervised classifications, randomly selecting a different subset of train areas each time. The total number of train sites for each land cover class must be higher than the number of train sites used for each classification and big enough for obtaining hundred different combinations of the train sites. In this study, a total of 519 training areas accounting for 46,346 pixels were selected from an aerial image of Murcia Region from year 2008 [17] using QGIS software [16]. For each classification 25-50% of each land cover class training areas were randomly selected.

In each classification a pixel might be assigned to different land cover classes, depending on the set of train areas selected. Hundred maps are therefore generated and later summarized into eleven maps — one for each land cover class, each of them representing the frequency of assignment of each pixel to a specific land cover class. The final land cover class assigned to a pixel in the resulting map will be ultimately the class which was more often assigned to this pixel (figure 5).

Spectral indices

Spectral indices for each Landsat image were calculated using *GRASS r.mapcalc* command and were included in the classification analysis as ancillary layers. These indices enhance the discrimination of vegetation, urban areas, bare soil and water bodies.

Normalised Difference Vegetation Index (NDVI) was calculated [45] using equation 1. NDVI is widely used in remote sensing studies for the identification of vegetation since it highlights photosynthetic activity [3]. NDVI normalizes values between -1 to +1. Dense vegetation shows high values, soil values are positive but lower, and water values are negative due to its strong absorption at NIR [22].

$$NDVI = \frac{NIR - R}{NIR + R} \quad (1)$$

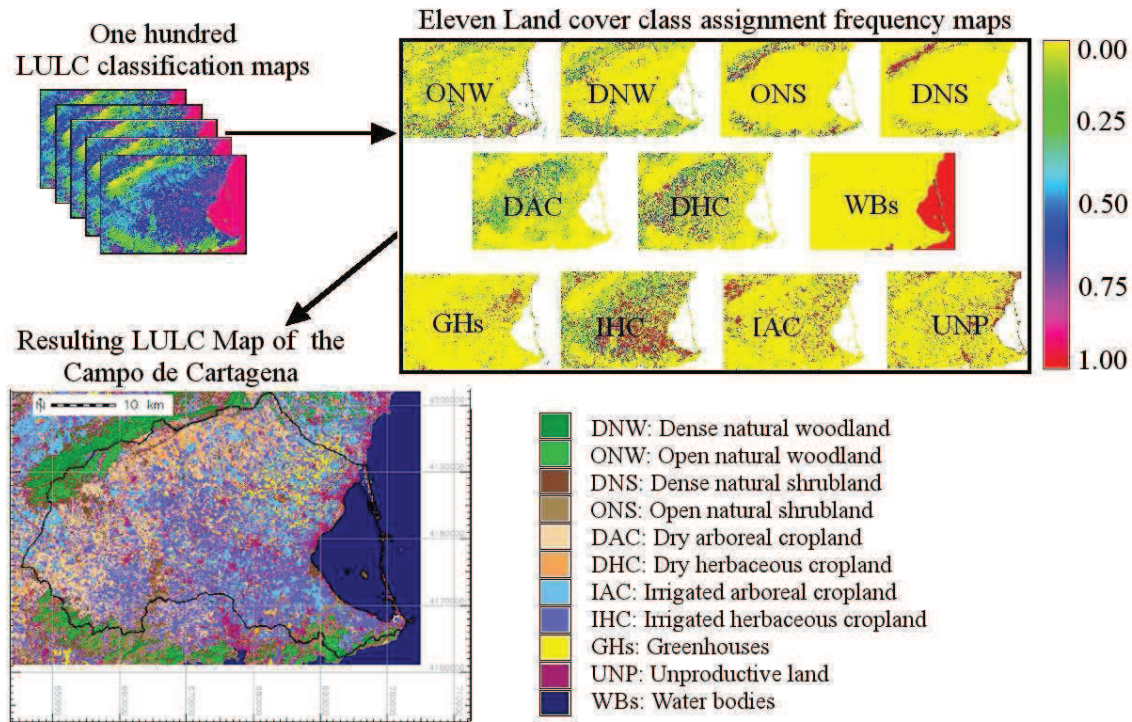


Figure 5. Land cover class assignment procedure.

The MNDWI (Modified Normalized Water Index) [29] was calculated to delineate water bodies and enhance its presence in remotely sensed imagery. It can also remove shadow effects on water, which are otherwise difficult to detect.

$$MNDWI = \frac{G - MIR}{G + MIR} \quad (2)$$

The NDBI (Normalized Difference Built-up Index) [49] was calculated to enhance the discrimination of built-up areas.

$$NDBI = \frac{NIR - MIR}{NIR + MIR} \quad (3)$$

Finally, we calculated the NDBaI (Normalized Difference Bareness Index) [9]. This index retrieves bare land from the Landsat images. Bare land (including beaches, bare land, and land under development) could be distinguished by NDBaI values higher than zero.

$$NDBaI = \frac{NIR - TIR}{NIR + TIR} \quad (4)$$

Shape indices

Landscape consists of several land cover class patches, often bigger than image pixel size. Landscape patches can automatically be delineated from images by means of several segmentation and edge detection algorithms. Land use/land cover classes tend to have different and sometimes very distinctive shapes. Anthropic areas tend to be more geometric than natural areas, greenhouses tend to be rectangular, roads tend to be elongated, etc.

Prior to classification, landscape patches in the study area were extracted by means of an automatic image segmentation algorithm. Two shape indices for each obtained patch were then calculated and scores were assigned to pixels belonging to each patch. The new maps with each corresponding shape index values were included in the classification as ancillary layers, hence including patch information at pixel scale.

Automatic segmentation was performed on a single Landsat scene using *SPRING 5.1.5* software [6]. *Region Growing* data grouping technique was performed on image bands number 1 to 7 (excluding the thermal infrared band). Similarity threshold (ranging from 0 to 100%) and minimum patch size (in image pixels units) parameters were set to 20 and 100 respectively, after several tries. Patches from the resulting map were scored according to the shape indices using *GRASS r.mapcalc* command. Two new maps were obtained based on Fractal Dimension (FD, equation 5) and Shape Index (SI, equation 6) of patches [10] (figure 6).

$$FD = \frac{2 \log_e(0.25p_i)}{\log_e(a_i)} \quad (5)$$

$$SI = \frac{0.25p_i}{\sqrt{a_i}} \quad (6)$$

Where a_i and p_i stand for the area and the perimeter of the patch i respectively.

In summary, input data for the classification analysis were the resulting shape and spectral indices maps, together with the single bands of the two Landsat scenes except for the thermal infrared band, which was not included in the analysis.

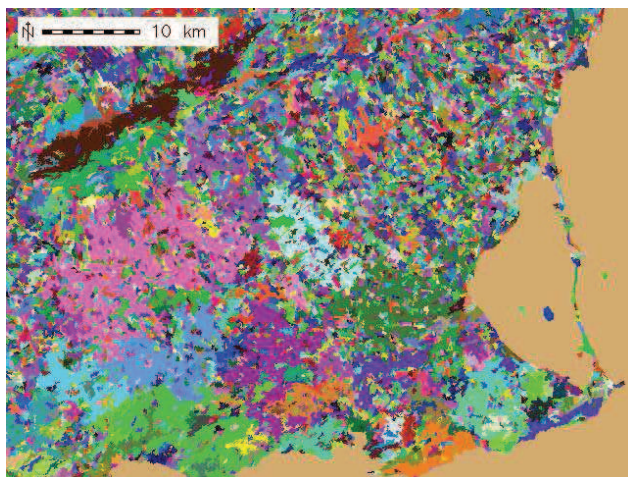


Figure 6. Automated landscape patches map obtained with *SPRING* software.

Validation

The methodology was verified by aerial image validation and stratified random sampling by land cover class. The number and proportion of pixels used to validate each land cover class was according to the training map.

An error matrix [11, 21] was generated to characterize the error associated to the classification and to compute several accuracy coefficients. User's and producer's accuracy parameters were calculated for each land cover class. These parameters respectively measure the commission error, defined as including an area in a category when it does not belong to that category, and the omission error, which is excluding an area from the category to which it belongs [11, 14]. The whole procedure is assessed with the overall accuracy (percentage of sampled pixels which are well classified) and the Kappa coefficient, which measures the degree of adjustment explained by the classification accuracy, after removing that attributed to random effects [21, 27, 28, 35].

Figure 7 summarizes the methodology applied.

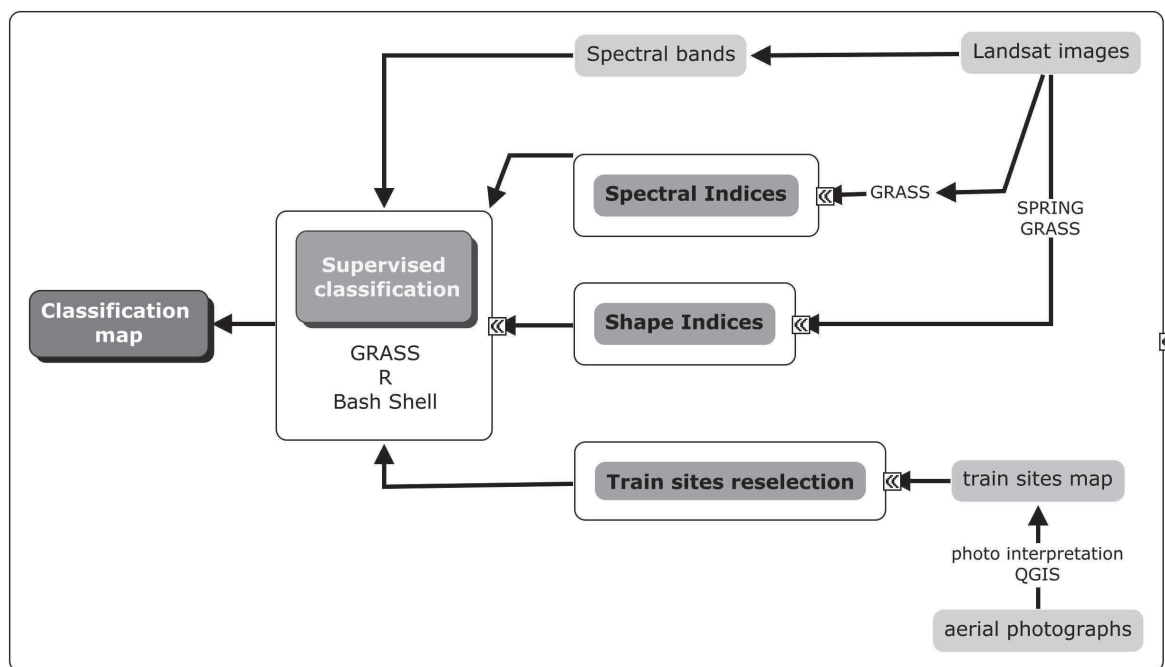


Figure 7. Conceptual diagram of the supervised classification methodology.

Results

A land-cover map was obtained for the Campo de Cartagena area and Marina del Carmolí wetland watershed boundaries were overlaid on this map to calculate land-cover class percentages (figure 8).

Overall accuracy percentage of sampled pixels which are well classified reached 83.14% with a Kappa value of 0.81. Land cover classes obtaining higher accuracies were DNW, DNS, IAC, OHC, GHs, UNP and WBs (table 1).

We tested the same classification without performing the train sites reselection procedure (TSR) and excluding the shape indices layers (SHI) and the overall accuracy and Kappa values obtained were of 78.09% and 0.75 respectively. Performing TSR without SHI showed an overall accuracy and Kappa values of 80.19% and 0.77 respectively. Thus, standard accuracy measures increased using these methods. TSR clearly improves the proper

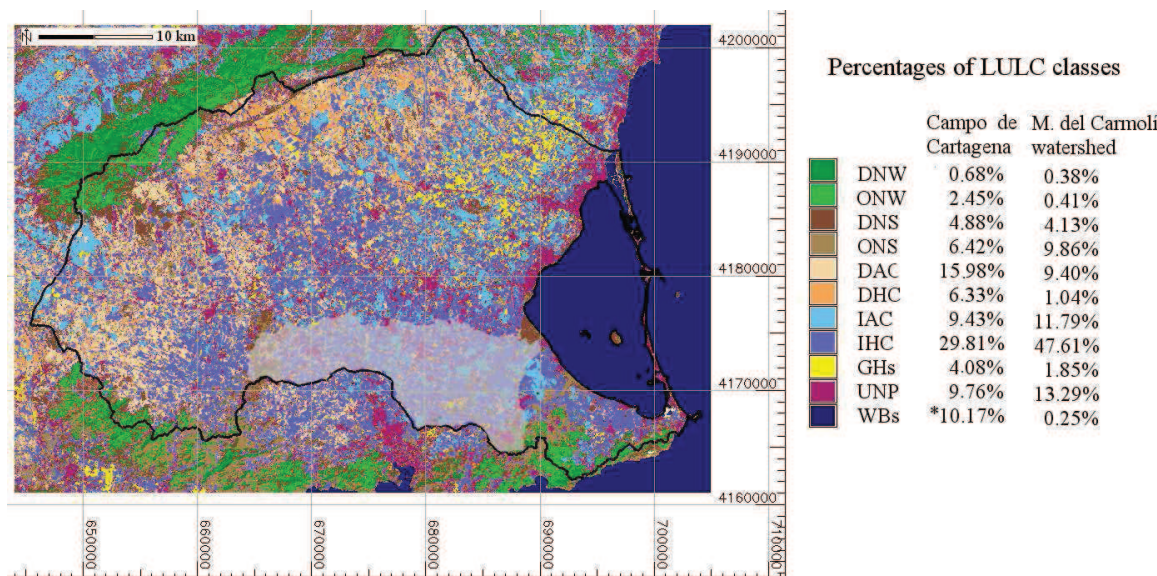


Figure 8. LULC map of Campo de Cartagena. The Marina del Carmolí watershed is overlaid in white color. Abbreviations are in the text. *WBs** include inland water bodies and the Mar Menor lagoon.

classification of pixels (figure 9b) in relation to the standard method (figure 9a) and the inclusion of shape indices (figure 9c) results in more compact landscape patches.

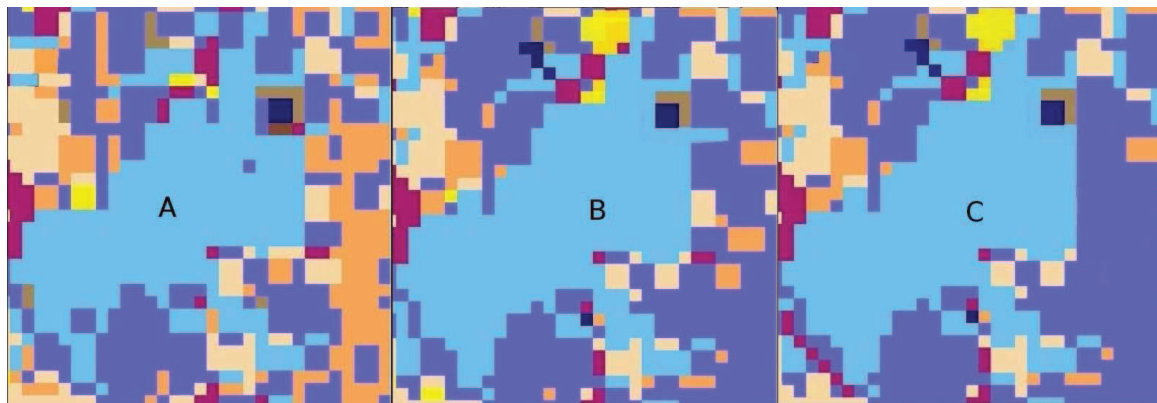


Figure 9. Detail of classification maps using different methodologies: (A) SPI (including spectral indices), (B) SPI+TSR, (C) SPI+TSR+SHI. Leyend of LULC classes is in figure 5 and abbreviations are explained in the text.

With the proposed methodology, landscape patches are much better identified and higher accuracies are obtained in the resulting LULC classification map. However, standard accuracy measures do not sufficiently reflect this enhancements since they are pixel based.

Table 1. Accuracy coefficients (%) of supervised classification map for each land cover class. Abbreviations are explained in the text.

	<i>User's accuracy</i>	<i>Producer's accuracy</i>
DNW	80.80	86.79
ONW	54.87	82.01
DNS	78.24	69.38
ONS	70.03	51.32
DAC	48.23	79.90
DHC	50.79	85.16
IAC	93.83	88.75
IHC	88.59	69.26
GHs	91.59	93.90
UNP	91.20	95.21
WBs	100.00	98.26

Wetland Plant Communities Mapping

Plant communities can be studied in order to assess wetland condition and can be tracked by means of remote sensing over time at different spatial scales. Characteristic plant communities of Marina del Carmolí wetland were first identified by means of ordination analysis of plant species cover data, obtained through systematic fieldwork sampling. Wetland plant communities were then mapped by means of remote sensing techniques using satellite and airborne images. Our aim was to develop a framework for the systematic characterization of wetland plant communities, as well as to compare the suitability of different sensors in terms of accuracy, spatial and temporal resolution for mapping Mediterranean semiarid wetlands [26, 39].

Plant communities characterization

Field sampling

Twelve representative perennial taxa were studied, i.e. *Arthrocnemum glaucum*, *Limonium cossonianum*, *Limonium caesium*, *Tamarix canariensis*, *Phragmites australis*, *Juncus maritimus*, *Plantago crassifolia*, *Lygeum spartum*, *Sueda vera*, *Frankenia corymbosa*, *Sarcocornia fruticosa* and *Halimione portulacoides*. A total of 550 georeferenced sampling units were surveyed in Marina del Carmolí wetland in June 2008, consisting of 4 m² areas regularly located within the wetland (figure 10). At each sampling unit, species abundance was recorded (0-100%), together with non wetland species and bare soil cover.

Statistical analyses

Taxa only occurring in less than 5% of the sampling units were discarded from the analysis. Final data matrix contained 470 sampling points. *Correspondence analysis* (CA) [4] was performed on the species-abundance matrix using *R* function *CA* from the FactoMineR



Figure 10. Field sampling units.

package [30]. *K-means* clustering [36] into ten groups was applied to the coordinates of the CA axes comprising most variability. The resulting centroid matrix of these groups was then transformed into a dissimilarity matrix using *R* function *dist* and *euclidean* distance. We used *R* function *hclust* to perform hierarchical cluster analysis and *R* function *cutree* to obtain a classification in 3 groups corresponding to salt steppe, salt marsh and reed beds communities. *R* function *indval* [44] was ultimately used to determine indicator species of each plant community type (table 2).

Table 2. Species indicator value for each community type after IndVal analysis.

Species	Indicator value	Community
<i>P. australis</i>	0.94	Reed beds
<i>H. portulacoides</i>	0.57	Salt marsh
<i>S. fruticosa</i>	0.55	Salt marsh
<i>S. vera</i>	0.48	Salt marsh
<i>A. glaucum</i>	0.29	Salt marsh
<i>L. spartum</i>	0.61	Saline Steppe
<i>F. corymbosa</i>	0.51	Saline Steppe
<i>P. crassifolia</i>	0.43	Saline Steppe

Non Metric Multi Dimensional Scaling was also performed using *R* function *metaMDS* [38] to represent obtained plant communities (figure 11).

Plant communities image mapping

Plant community maps of the Marina del Carmolí wetland were obtained by means of supervised classification of image using two different sensors. Airborne sensor images were captured in June 2008 within the NATMUR-08 project [17]. The airborne sensor used was a *DMC Z/I Intergraph* camera with resolution in four spectral bands, *i.e.* red (R, 590-675 nm), green (G, 500-650 nm), blue (B, 400-580 nm) and near infrared (NIR, 675-850 nm), and a pixel size of 2 meters. Normalised Difference Vegetation Index (NDVI) was calculated [45] using equation 1 and was included as an ancillary layer in classification analysis.

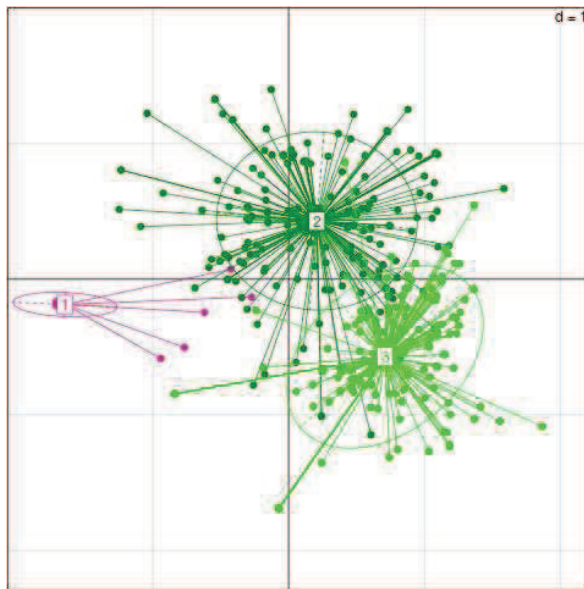


Figure 11. Non metric multidimensional scaling performed on the species distance matrix. Dots correspond to sampling units. Salt marsh community is denoted in dark green (2), salt steppe is in light green (3) and reed beds in purple (1).

Classification was performed in two steps. First, unsupervised classification was used to identify areas belonging to infrastructures, water bodies and open spaces of bare soil. For this purpose, *GRASS* command *i.cluster* was performed to obtain 20 automatic classes, from which non vegetation categories were identified. Results were visually validated using aerial photography. A total of 12 ha of bare soil open spaces were identified in the image, 10 ha of infrastructures and 0.78 ha of water bodies. These pixels were excluded from further identification of plant communities.

Georeferenced sampling points (2x2 m) previously obtained in the field were used as training and validation areas. For airborne image classification fifty percent of the pixels belonging to each plant community type was randomly selected and assigned to the training and validation maps respectively. *GRASS* command *r.random* was used for this purpose. Pixel size of training and validation areas was doubled to 4x4 m in order to account for potential errors in the accuracy of the GPS device used in the field. Sampling units used as training and validation areas comprised 0.33 ha and 0.36 ha respectively. For Landsat image classification train and validation sites were manually digitized creating polygons over several field sampling units of the same category. This was necessary because size of single sampling units was much smaller than pixel size resolution of Landsat images.

GRASS classification algorithm used is based on maximum likelihood [11, 21] and was performed using the *i.maxlik* command. Classification of airborne sensor images was enhanced with the train sites reselection method described in the previous chapter.

Classification results were validated and assessed by means of the Kappa [13] and overall accuracy parameters, which reached 0.61 and 74.45% respectively for the airborne image classification and 0.61 and 74.67% respectively for the Landsat image classification. Tables 3 and 4 show the error matrix of the airborne and Landsat based classifications respectively.

Table 3. Error matrix of the airborne sensor classification.

User's accuracy		Producer's accuracy
SE	75.35%	96.07%
SM	81.93%	62.62%
RB	62.16%	69.00%
Overall accuracy		Kappa
74.45%		0.61

Table 4. Error matrix of the Landsat sensor classification.

User's accuracy		Producer's accuracy
SE	68.60%	71.00%
SM	80.22%	70.48%
RB	72.22%	83.57%
Overall accuracy		Kappa
74.67%		0.61

Figure 12 shows both resulting classification maps.

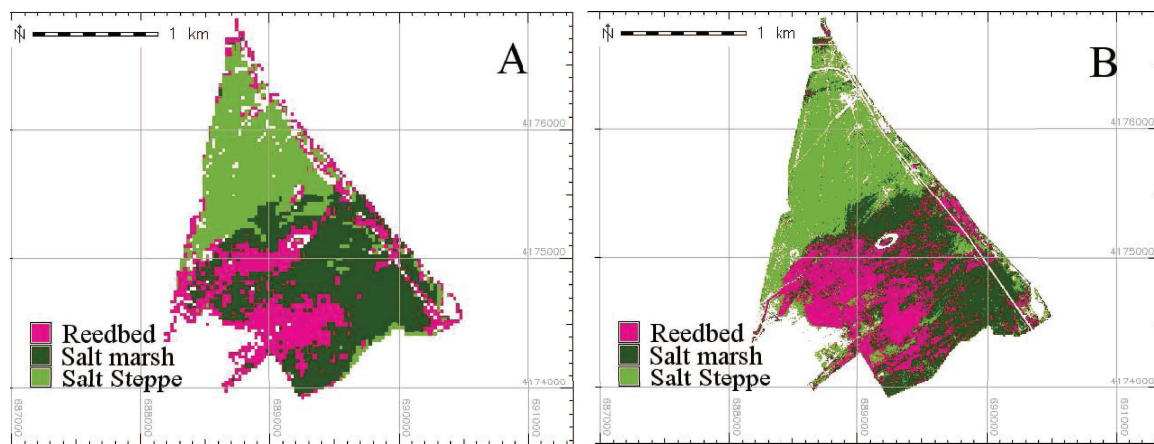


Figure 12. Plant community maps obtained with Landsat (a) and airborne (b) classification at 25 and 2 meters resolution respectively.

Although overall classification accuracy is almost identical using each remote sensor, areas occupied by plant communities and their accuracies vary (table 5). Major differences appear in the area occupied by salt marsh and salt steppe communities. Reed beds community obtains almost identical values in both classifications. Landsat based classification seem to underestimate smaller salt steppe patches which are embedded in salt marshes or reed beds communities. Although Landsat spectral resolution is higher, spatial resolution is much lower. Plant communities maps obtained using Landsat imagery must focus on more general communities occupying bigger areas, whereas airborne sensors can be used to map

small patches of more discrete plant communities. However, Landsat imagery is regularly available from the seventies onwards, which makes it very useful for historical studies on plant community changes during time [8].

Table 5. Area occupied by each plant community using both sensors (hectares).

	Landsat sensor	Airborne sensor
Salt Steppe	91.07	109.44
Salt Marsh	115.52	99.69
Reed bed	79.55	77.24

Conclusion

According to our results, the watershed delineation methodology proposed here showed a great improvement compared to the standard watershed modelling procedure. It is specially suitable for wetlands located in plain areas.

The method proposed for remote sensing of land use/land cover classes is easily automated by means of bash scripts. The use of ancillary layers, the inclusion of patch scale information and the iterative random reselection of train sites procedure resulted in maps with greater accuracies and with more compact landscape patches. Moreover, accuracy dramatically increased in LULC classification analysis performed on a historical set of Landsat images using this methodology [7]. Since older aerial photographies have lower resolution, reliable train sites are more difficult to obtain, and therefore the random reselection method helps in overcoming image quality.

Plant communities are not discrete entities and their species composition vary across wetlands based on wetland type, water table level, soil and water physicochemical conditions, etc. They can be used as proxies for assessing wetland condition status. The proposed systematic procedure for characterizing and mapping wetland plant communities is therefore an accurate tool for wetland study and management. This methodology can be easily replicated using different remote sensors, making it a flexible methodology for wetland plant communities mapping at different scales.

This set of GIS methodological tools is specifically adapted for monitoring wetlands and watershed condition and allows to further relate watershed scale pressures and wetland plant communities over time and at different spatial scales. Results support the applicability of free open source software for this kind of studies, thus facilitating replicability and making it an inexpensive methodology.

Acknowledgements

Financial support was provided by the project "Estado Ecológico de los Humedales Mediterráneos Semiáridos: Propuesta de Indicadores para su Evaluación" (I+D N°: CGL2006-08134) and a FPI grant. We thank the Spanish "Plan Nacional de Teledetección" project and the "NATMUR-08" project of the Murcia Region Authorities for the image data.

References

- [1] T. K. Alexandridis, G. C. Zalidis, and N. G. Silleos. Mapping irrigated area in mediterranean basins using low cost satellite earth observation. *Computers and Electronics in Agriculture*, 64(2):93–103, 2008.
- [2] R. Ballester, M. R. Vidal-Abarca, M. A. Esteve, M. L. Suárez, R. Gómez, and F. Robledano. *Los humedales de la Región de Murcia: Claves para su interpretación*. Consejería de Agricultura, Agua y Medio Ambiente. Dirección General del Medio Natural, Murcia, 2003.
- [3] A. Bannari, D. Morin, F. Bonn, and A. R. Huete. A review of vegetation indices. *Remote Sensing Reviews*, 13(1):95–120, 1995.
- [4] J. P. Benzécri. *L'analyse des données*. Dunod, Paris-Bruxelles-Montréal, 1973.
- [5] B. A. Bradley and J. F. Mustard. Identifying land cover variability distinct from land cover change: Cheatgrass in the great basin. *Remote Sensing of Environment*, 94(2):204–213, 2005.
- [6] G. Cámara, R. Souza, U. Freitas, and J. Garrido. Spring: Integrating remote sensing and gis by object-oriented data modelling. *Computers & graphics*, 20(3):395–403, 1996.
- [7] M. F. Carreño. *Seguimiento, con SIG y Teledetección, de los cambios de usos en la cuenca del Mar Menor, 1987-2009, y su influencia en los hábitats naturales y comunidades asociados*. PhD thesis, Murcia, in preparation.
- [8] M. F. Carreño, M. A. Esteve, J. Martínez, J. A. Palazón, and M. T. Pardo. Habitat changes in coastal wetlands associated to hydrological changes in the watershed. *Estuarine Coastal and Shelf Science*, 77(3):475–483, 2008.
- [9] X. L. Chen, H. M. Zhao, P. X. Li, and Z. Y. Yin. Remote sensing image-based analysis of the relationship between urban heat island and land use/cover changes. *Remote Sensing of Environment*, 104(2):133–146, 2006.
- [10] G. Chust, D. Ducrot, and J. L. Pretus. Land cover mapping with patch-derived landscape indices. *Landscape and Urban Planning*, 69(4):437–449, 2004.
- [11] E. Chuvieco. *Teledetección ambiental. la observación de la tierra desde el espacio*. Editorial Ariel, Barcelona, 1 edition, 2002.
- [12] C. Conesa. *El Campo de Cartagena: clima e hidrología en un medio semiárido*, volume 13 of *Cuadernos*. Universidad de Murcia, Murcia, 1 edition, 1990.
- [13] R. G. Congalton. A review of assessing the accuracy of classifications of remotely sensed data. *Remote Sensing of Environment*, 37(1):35–46, 1991.
- [14] R. G. Congalton and K. Green. Assessing the accuracy of remotely sensed data: Principles and practices. 2009.

- [15] J. K. Cronk and M. S. Fennessy. *Wetland plants: biology and ecology*. CRC, 2001.
- [16] Development Team. *Quantum GIS Geographic Information System. Open Source Geospatial Foundation Project*, 2009. <http://www.qgis.org/>.
- [17] Dirección General de Patrimonio Natural y Biodiversidad. Consejería de Agricultura y Agua. Comunidad Autónoma de la Región de Murcia. *NATMUR-08 project*, 2008. <http://www.murcianatural.com/natmur08/>.
- [18] DIRECTIVE, H.A.S.A.T. Council directive 92/43/eec of 21 may 1992 on the conservation of natural habitats and of wild fauna and flora. *Official Journal L*, 206(22/07):0007–0050, 1992.
- [19] M. A. Esteve, M. F. Carreño, F. Robledano, J. Martínez-Fernández, and J. Miñano. *Dynamics of Coastal Wetlands and Land Use Changes in the Watershed: Implications for the Biodiversity*, chapter 4, pages 133–175. Nova Science Publishers Inc, Hauppauge New York, 2008.
- [20] European Commission. Directorate-General for Environment. *Interpretation manual of European Union habitats*. European Commission, DG Environment, 2007.
- [21] G. M. Foody. Status of land cover classification accuracy assessment. *Remote Sensing of Environment*, 80(1):185–201, 2002.
- [22] E. P. Glenn, A. R. Huete, P. L. Nagler, and S. G. Nelson. Relationship between remotely-sensed vegetation indices, canopy attributes and plant physiological processes: What vegetation indices can and cannot tell us about the landscape. *Sensors*, 8(4):2136–2160, 2008.
- [23] J. C. González. *Propuesta de un método eficiente y de bajo coste para la elaboración de mapas de cultivos mediante imágenes Landsat. El caso de los cítricos en la Región de Murcia (España)*. PhD thesis, Murcia, 2011.
- [24] GRASS Development Team. *Geographic Resources Analysis Support System Software*, 2008. <http://grass.fbk.eu/>.
- [25] T. P. Hollenhorst, T. N. Brown, L. B. Johnson, J. J. H. Ciborowski, and G. E. Host. Methods for generating multi-scale watershed delineations for indicator development in great lake coastal ecosystems. *Journal of Great Lakes Research*, 33(3):13–26, 2007.
- [26] N. Horning, J. A. Robinson, E. J. Sterling, W. Turner, and S. Spector. *Remote Sensing for Ecology and Conservation: A Handbook of Techniques*. Oxford Univ Press, 2010.
- [27] L. Hubert-Moy, A. Cottonec, L. Le Du, A. Chardin, and P. Perez. A comparison of parametric classification procedures of remotely sensed data applied on different landscape units. *Remote Sensing of Environment*, 75(2):174–187, 2001.
- [28] W. D. Hudson. Evaluating landsat classification accuracy from forest cover-type maps. *Canadian Journal of Remote Sensing*, 13(1):39–42, 1987.

- [29] F. Hui, B. Xu, H. Huang, Q. Yu, and P. Gong. Modelling spatial-temporal change of poyang lake using multitemporal landsat imagery. *International journal of remote sensing*, 29(19-20):18, 2008.
- [30] F. Husson, J. Josse, S. Le, and M. J. *FactoMineR: Multivariate Exploratory Data Analysis and Data Mining with R*, 2010. R package version 1.14.
- [31] C. A. Johnston, J. B. Zedler, M. G. Tulbure, C. B. Frieswyk, B. L. Bedford, and L. Vacarro. A unifying approach for evaluating the condition of wetland plant communities and identifying related stressors. *Ecological Applications*, 19(7):1739–1757, 2009.
- [32] K. Jones, Y. Lanthier, P. van der Voet, E. van Valkengoed, D. Taylor, and D. Fernández-Prieto. Monitoring and assessment of wetlands using earth observation: The globwetland project. *Journal of environmental management*, 90(7):2154–2169, 2009.
- [33] R. S. King, M. E. Baker, D. F. Whigham, D. E. Weller, T. E. Jordan, P. F. Kazyak, and M. K. Hurd. Spatial considerations for linking watershed land cover to ecological indicators in streams. *Ecological Applications*, 15(1):137–153, 2005.
- [34] T. M. Lee and H. C. Yeh. Applying remote sensing techniques to monitor shifting wetland vegetation: A case study of danshui river estuary mangrove communities, taiwan. *Ecological Engineering*, 35(4):487–496, 2009.
- [35] C. Liu, P. Frazier, and L. Kumar. Comparative assessment of the measures of thematic classification accuracy. *Remote Sensing of Environment*, 107(4):606–616, 2007.
- [36] S. P. Lloyd. Least squares quantization in pcm. *IEEE Transactions on Information Theory*, 28:128–137, 1982.
- [37] D. B. Michelson, B. M. Liljeberg, and P. Pilesjö. Comparison of algorithms for classifying swedish landcover using landsat tm and ers-1 sar data. *Remote Sensing of Environment*, 71(1):1–15, 2000.
- [38] J. Oksanen, G. Blanchet, R. Kindt, P. Legendre, R. B. O'Hara, G. Simpson, P. Solymos, S., and H. Wagner. *vegan: Community Ecology Package*, 2011. R package version 1.17-8.
- [39] S. Ozesmi and M. Bauer. Satellite remote sensing of wetlands. *Wetlands Ecology and Management*, 10(5):381–402, 2002.
- [40] B. Poulin, A. Davranche, and G. Lefebvre. Ecological assessment of phragmites australis wetlands using multi-season spot-5 scenes. *Remote Sensing of Environment*, 114(7):1602–1609, 2010.
- [41] B. Prenzel. Remote sensing-based quantification of land-cover and land-use change for planning. *Progress in Planning*, 61(4):281 – 299, 2004.
- [42] R Development Core Team. *R: A Language and Environment for Statistical Computing*. R Foundation for Statistical Computing, Vienna, Austria, 2011. ISBN 3-900051-07-0.

- [43] J. A. Richards and X. Jia. *Remote Sensing Digital Image Analysis: An Introduction*. Springer, 4th edition, 2006.
- [44] D. Roberts. *labdsv: Ordination and Multivariate Analysis for Ecology*. 2010. R package version 1.4-1.
- [45] J. W. Rouse, R. H. Haas, J. A. Schell, and D. W. Deering. Monitoring vegetation systems in the great plains with erts. In *Proceedings of the Third ERTS Symposium*, volume 1, pages 309–317. NASA, 1973.
- [46] C. Song, C. E. Woodcock, K. C. Seto, M. P. Lenney, and S. A. Macomber. Classification and change detection using landsat tm data: When and how to correct atmospheric effects? *Remote Sensing of Environment*, 75(2):230–244, 2001.
- [47] S. T. Y. Tong and W. Chen. Modeling the relationship between land use and surface water quality. *Journal of Environmental Management*, 66(4):377–393, 2002.
- [48] P. Wolter, C. Johnston, and G. Niemi. Land use land cover change in the us great lakes basin 1992 to 2001. *Journal of Great Lakes Research*, 32(3):607–628, 2006.
- [49] Y. Zha, J. Gao, and S. Ni. Use of normalized difference built-up index in automatically mapping urban areas from tm imagery. *International Journal of Remote Sensing*, 24(3):583–594, 2003.